Thermoluminescence Properties of Bioglass for Radiation Dosimetry

Huda A. Alazab
EAEA: Egyptian Atomic Energy Authority
N.Y. Abdou
EAEA: Egyptian Atomic Energy Authority
H. A. Saudi
Al-Azhar University
wesam Abd-Allah (wesamomar2007@yahoo.com)
National Center of Radiation Research & Technology Atomic Energy Authority https://orcid.org/0000-0003-4745-4344

Research Article

Keywords: Thermoluminescence, Hench's Bioglass, XRD, Dose- Response

Posted Date: June 14th, 2021

DOI: https://doi.org/10.21203/rs.3.rs-574661/v1

Abstract

The thermoluminescence technique was employed to study bioglass matrices prepared using the traditional technique of glass making. The synthesized bioglass matrices were investigated using X-ray diffraction (XRD), and differential thermal analysis (DTA) has been studied. The highest thermoluminescent intensity was found for the bioglass matric of 26.91% CaO, 46.134% SiO_2, 2.60% P_2O_5, 24.34%Na_2O (mol%), with only one glow peak at 460 k. The TL response illustrations linearity in high gamma dose range from 25 to 1000 Gy. This new bioglass matric might become useful in high-dose fields for dosimetry.

1. Introduction

Since the mid 1980's, bioglass began to be used in medical applications such as bone regeneration(1; 2). In bioglass exposed to ionizing radiation, electron-hole and recombination processes are rich in interesting mechanisms involving charge and energy transfer between populations of specific impurities and defects (3) .

Thermoluminescence (TL) is a massive technique for investigating the origin of defects in solid materials (4). High radiation exposures acquired throughout a several applications, such as those in nuclear power plants, food irradiation, radiotherapy, and medical device sterilization, maybe an exciting field of research. The development of amorphous systems is therefore critical for this particular application (5; 6).

New silicate materials with improved sensitivity and linearity of TL performance over a wide range of dosages are currently being developed (1–4).

A large amount of research literature has also been dedicated to analyses of glass's radiation hardness in terms of its response to UV light, X-rays, □-rays, electrons, and neutrons. Many defects that contribute to the formation of structural models have been identified in the past. The study of radiation-induced glass defect centers has become a common research subject in recent years, as such studies aid in determining the suitability of glasses for radiation dosimetry applications. The effect of gamma rays on amorphous material such as glass is to generate secondary electrons from the positions where they are in a stable state with additional energy. These excited electrons migrate through the glass network and are eventually captured, forming color centers, depending on their energy and the structure of the glass. Metal cations that make up the surface of the glass may be the trapping sites. Ions of admixtures to the key structural defects of the composition or owing to impurities in the glass structure (7).

As a result, the focus of this research is on using bioglass to investigate TLD dosimetry. Glow curve profiles, TL sensitivity, and dose-response were among the physical parameters investigated. The findings could help in the development of TL detectors that can tolerate a large variety of radiation exposures.

2. Methodology

The samples were prepared from various mol percentages of the following compositions (1) 29.13% CaO, 44.49% SiO2, 26.36%Na2O; (2) 26.91% CaO, 46.134% SiO2, 2.60% P2O5, 24.34%Na2O; (3) 23.92% CaO, 51.5% SiO2, 2.90% P2O5, 21.64%Na2O; (4) 23.58% CaO, 2.13% SiO2, 2.94% P2O5, 21.33%, Na2O (mo%) for G1, G2, G3, and G4, respectively by the traditional technique of glass making.

To verify the status of fabricated glasses, the Shimadzu X-ray diffractometer carried out at 40 kV and 30 mA was used.

Temperature characteristics, such as glass transition T_g, crystallization initiation T_x and melting temperature T_m (Netzch STA 409 simultaneous thermal Analyzer, DTA / T_G mode, ± 2ºC) with 283 k/min rate for heating were determined. In all DTA / T_G runs, synthetic air atmosphere (20 percent O_2 and 80 percent N_2) and an Aluminum oxide crucible as a guide was used. ΔT was obtained by $\Delta T = T_x - T_{g1}$, which was defined as the thermal stability against devitrification.

Bioglass samples of G1, G2, G3, and G4 are irradiated to differing gamma doses ranging from 0.25 Gy to 1000 Gy using a ^{60}Co irradiation cell-220 (GC220) source manufactured by the Atomic Energy of Canada with dose rate of 0.3 Gy/sec, this gamma source is available at the National Center for Radiation Research and Technology in Cairo, Egypt.

Harshaw Model 3500 TLD Reader was used to test the samples. The reader is operated by the WinREMS program, which runs on a computer that is connected to the reader. The glow curves of the samples were estimated from 323 K to 673 K at a linear heating rate of 5 k/sec., the background was subtracted from all results by taking the reading from each sample before irradiation, then subtracts from the reading after irradiation.

3. Results And Discussion

3.1. Glass Characterization

The X-ray diffraction (XRD) pattern was used to confirm the formation of the synthesized compound. and the result are shown in **Fig. (1)** that proved that all of the samples are in a glassy state.

The study of thermal scanning of the glass is important because it provides information about the thermal properties of this glass in addition to some structure or phased transformations (8). DTA was used to check the characteristic temperatures, the glass transition temperature (T_g), crystallization (T_p) and melting temperatures when the glass heated, and its heat capacity. Other properties also change in a narrow temperature range, called the extent of transformation or the glass transformation where the structural molecules of the glass network acquire movement, which makes it possible to change. The first endothermic peak corresponds to the glass transition temperature (T_g). The exothermic peak follows the glass transition temperature that indicates the phase of crystallization temperature (T_p). The exothermic effect usually follows either one or several endothermic effects and is known as the melting temperature

(T_m). Figure (2**)** shows the results of the DTA obtained, and the mixed alkali and alkaline elements effect added to the glass matrix shows a clear deviation. It turns out that the value of T_g varies from one sample to another.

Figure (3) shows the glass transition temperature values, T_g, of the glass samples, which increase slowly as the alkali and alkali earth elements oxide mixture content increases, i.e. the structural connectivity increases. In addition, T_g relies on the BO_3 and BO_4 groups, adding to the compactness of the structure and an improvement in the temperature of T_g temperature.

The thermal stability of the glasses is the result of a glass structure, which has a closely supported structure. Conversely, the thermally unstable glasses frame has a loose packaging.

The stability of the glass showed a difference and decreases with a decreasing the silicon ratio and a change in the proportions of the mixture of alkali and alkali earth elements in the composition of the bioglass, which indicates that the homogeneity of the glass changes with the composition G3 (23.92% CaO, 51.5% SiO_2, 2.90% P_2O_5, 21.64%Na_2O), and this is in line with the infrared spectra and density.

3.2. Thermoluminescence study

The radiation dosimetric achievement of a TL material strongly relies on the structure of its glow curve, such as maximum TL- intensity, and position of glow peaks [1]. So, after exposure to the test dose (50 Gy from gamma-ray), the TL glow curves of G1, G2, G3, and G4 were studied, and the findings are shown in **Fig. (4)**. It can be seen in the figure that G1, G2, G3, and G4, have the same shape of glow curves which indicated that these glasses contain the same types of traps. Hole traps are formed by non-bridging oxygen defects and fused silica, while electron traps are formed by empty Si and Na orbitals (9; 10).

while the glow curves for G1, G2, G3, and G4 are identical in form, the TL-intensities and peak position are dissimilar, as seen in **Fig. (5)**. this figure clearly shows that G2 has the highest TL-intensity, followed by G1, G3, and G4, in that order. G1 and G2 have the same chemical composition except G2 contain 6% from P_2O_5 which may be responsible for the production of more electron traps in G2 than G1. The difference of TL- intensity between different types of glass may be due to the presence of different amounts from the chemical composition of the glass (SiO_2, Na_2O, CaO, P_2O_5, TiO_2).

Also, the peak positions for G1, G2, G3, and G4, respectively, are different. The peak position for G1 at 454 K, G2 and G4 at 460 K, and G3 at 470 K. According to previous studies, the ideal glow curve for glass should have a single peak with maximum temperature between 453, and 523 K. (11; 12). Figure (6**)**: Shows the glow curves of G1, G2, G3, and G4 respectively after irradiated with different gamma doses from 0.25 to 1000 Gy. For all doses, there are slight differences in the peak temperatures for all the bioglass matrices. However, with rising radiation dose, the TL-Intensity in all bioglass forms increases. This means that as the radiation exposure raises, the number of active traps increases, corresponding to a rise in the number of recombination traps, resulting in an increase in TL-Intensity when reading the bioglass samples. (13; 14).

3.3. Repeatability of TL measurements

One of the most important characteristics to be met in any dosimeter is the accuracy of this dosimeter with reuse. The coefficient of variation (CV) of TL-response for a particular dosimeter that undergoes the same treatment should not exceed ± 7.5% (15; 16). Therefore, all bioglass samples were subjected to cycles of irradiation at test dose (50 Gy), readout, and annealing to test its repeatability and (CV) was obtained by using Eq. (1):

$$CV = 100\left(\frac{SD}{M}\right) \quad (1)$$

Where, the average of the readouts is m, and the standard deviation is SD.

The CV values for G1, G2, G3, and G4 were found to be 6.7%, 5.3%, 6.3%, and 2.2% respectively, which are lower than the recommended value (7.5%) in all bioglass types.

3.4. Dose response

The linearity of the relation between irradiation dose and TL- intensity is one of the most critical features about any dosimeter, since it defines the range of radiation dose for a dosimeter. the supralinearity index F(D), is a tool to estimate a material's linearity, which first introduced by **Horowitz (1981)** and **Mische and McKeever (1989)**(4; 17–19)using the Eq. (2):

$$F(D) = \frac{f(D)/D}{f(D_1)/D1} \quad (2)$$

Where, f(D) is the TL- intensity at a low dose 'D', and f(D1) is the TL intensity at a high dose 'D_1', the supralinearity index F(D) is equal to one within linear region, F(D) is higher than one within supralinear region and F(D) is lower than one within sublinear region. It was found that in the case of G1, G3, G4, the dose-response curves were sub-linear from 1 up to 25 Gy and become linear from 100 up to 1 kGy. However, in the case of G2, it was sub- linear from 1 up to 10 Gy and become linear from 25 up to 1 kGy as shown in **Table (1).** The dose-response for G1, G2, G3, and G4, respectively are shown in **Fig. (7**). **Table (2)** shows the linear dose range for the present bioglass matrixes types and those of previous works(20–23).

3.5. Kinetic analysis

Deconvolution functions for general orders of kinetics derived by **kities, et al.**, (24) have been used to determine kinetic parameters such as activation energy and frequency factor, and the result of deconvolution for G1, G2, G3, and G4, respectively are seen in **Fig. (8**). **Table (3)** shows the activation energies and frequency factories for G1, G2, G3, and G4 respectively.

The kinetic parameters also have been determined by the peak shape according to Chen method (9; 15) and the result is shown in **Table (4).**

From these results, it can be observed that there is an agreement between activation energies and frequency factories calculated by two methods.

4. Conclusion

This work aims at studying thermoluminescence properties of four matrices derived from Hench's Bioglass with different molar ratios. It has been found that these matrices have the same shape of glow curve, but differ only in TL-intensity. The bioglass matrix (G2) has the highest TL-Intensity, then G1, G3, and G4 respectively. The linear gamma dose-response ranged from 100 up to 1000 Gy for all matrices, except G2, which has gamma dose-response from 25 up to 1000 Gy. A variability coefficient (CV) equal to 6.7%, 5.3%, 6.3%, and 2.2% for G1, G2, G3, and G4 respectively. Depending on these findings, the new bioglass matrix was thought to be a suitable material for potential use as a high-dose thermoluminescent dosimeter.

Declarations

Author contributions: The authors have equal contribution in the paper.

Acknowledgments: The authors thank the National Center for Radiation Research and Technology, Egyptian Atomic Energy Authority, Nuclear and Radiological Regulatory Authority, Egypt for the possibility to use their equipment and facilities

Availability of data and material: My manuscript and associated personal data will be shared with Research Square for the delivery of the author dashboard.

Compliance with ethical standards: The manuscript has not been published elsewhere and has not been submitted simultaneously for publication elsewhere.

Conflict of interest: The authors declare that they have no conflict of interest.

Declaration of Competing Interest: The authors declare that they have no known competing financial interests or personal relationships that could have appeared to influence the work reported in this paper.

Funding statement: There are currently no Funding Sources on the list

Consent to participate: The authors consent to participate.

Consent for Publication: The author's consent for publication.

References

1. Groh D, Döhler F, Brauer DS (2014) Acta biomaterialia 10:4465–4473
2. Jones JR (2013) Acta biomaterialia 9:4457–4486

3. Da Costa Z, Melo AP, Giehl J, Ludwig V, Pontuschka W, Caldas LV (2007) physica status solidi c 4:1118–1121
4. Shivaramu N, Lakshminarasappa B, Nagabhushana K, Swart H, Fouran S (2018) Spectrochim Acta Part A Mol Biomol Spectrosc 189:349–356
5. Chen R, Pagonis V (2011) Thermally and optically stimulated luminescence: a simulation approach. John Wiley & Sons
6. Thomas S, Chithambo M (2017) Radiat Eff Defects Solids 172:323–336
7. Marzouk S, Elalaily N, Ezz-Eldin F, Abd-Allah W (2006) Physica B 382:340–351
8. Singh SP, Pal K, Tarafder A, Das M, Annapurna K, Karmakar B (2010) Bull Mater Sci 33:33–41
9. McKeever SW (1988) Thermoluminescence of solids. Cambridge University Press
10. Chialanza MR, Keuchkerian R, Cárdenas A, Olivera A, Vazquez S et al (2015) J Non-Cryst Solids 427:191–198
11. Lim TY, Wagiran H, Hussin R, Hashim S (2015) Appl Radiat Isot 102:10–14
12. Thumsa-ard T, Laopaiboon R, Laopaiboon J (2017) J Lumin 181:286–290
13. Chowdhury M, Sharma S, Lochab S (2015) Mater Res Bull 70:584–589
14. Abdou N, Farag M, Abd-Allah W (2020) The European Physical Journal Plus 135:1–12
15. Furetta C (2010) Handbook of thermoluminescence. World Scientific
16. González P, Ávila O, Escobar-Alarcón L, Mendoza-Anaya D (2020) *Applied Radiation and Isotopes*:109174
17. Horowitz Y (1981) Phys Med Biol 26:765
18. Mische E, McKeever S (1989) Radiat Prot Dosimetry 29:159–175
19. Moscovitch M (1999) Radiat Prot Dosimetry 85:49–56
20. Kumar D, Bhatia V, Rao S, Chen C-L, Kaur N, Singh SP (2020) Mater Chem Phys 243:122546
21. Sanyal B, Goswami M, Shobha S, Prakasan V, Krishnan M, Ghosh SK (2019) J Lumin 216:116725
22. Alajerami Y, Mhareb M, Abushab K, Ramadan K (2019) Physica B 558:142–145
23. Saidu A, Wagiran H, Saeed M, Obayes H, Bala A, Usman F (2018) Radiat Phys Chem 144:413–418
24. Kitis G, Gomez-Ros J, Tuyn J (1998) J Phys D: Appl Phys 31:2636

Tables

Table 1. The Linear and sub-linear region for G1, G2, G3, and G4, respectively.

Glass ID	Linear Region		Sub-Linear Region	
	Range	*F(D)	Range	*F(D)
G1	100-1k Gy	1.02	1- 25 Gy	0.28
G2	25- 1k Gy	0.95	1- 05 Gy	0.51
G3	100-1k Gy	1.06	1- 25 Gy	0.16
G4	100-1k Gy	1	1- 25 Gy	0.33

*F(D): supra-linearity index.

Table 2. The linear dose range for present glass types and previous works

Glass ID	Range	References
G1, G3, and G4	100 Gy - 1kGy	Present work
G2	25 Gy - 1kGy	Present work
NaSrB : Nd^{3+}	5 Gy - 10 kGy	[26]
LB01	25 Gy - 5 kGy	[27]
NB:Dy, Li	1 Gy - 1 kGy	[28]
ZLB:Tb	0.5 Gy - 100 Gy	[29]

Table 3. The values of activation energies and frequency factories for G1, G2, G3, and G4 respectively using general orders of kinetics equation derived by **kities, et al., [9]** .

Glass ID	Tm (k)	E (eV)	S (s^{-1})	FOM %
G1	454	0.75	$4.1x10^{7}$	0.043
G2	460	0.70	$8.2x10^{6}$	0.037
G3	470	0.60	$3.9x10^{5}$	0.002
G4	460	0.80	$1.2x10^{8}$	0.041

Table 4. The values of activation energies and frequency factories for G1, G2, G3, and G4 respectively calculated by peak shape method.

Glass ID	Tm (K)	T_1 (K)	T_2 (K)	μ	E (ev)	S (s^{-1})
G1	454	415	492	0.49	0.76	4.78×10^7
G2	460	417.5	506	0.52	0.71	9.65×10^6
G3	470	421.6	518	0.50	0.60	3.55×10^5
G4	460	422	500	0.51	0.79	1.01×10^8

Figures

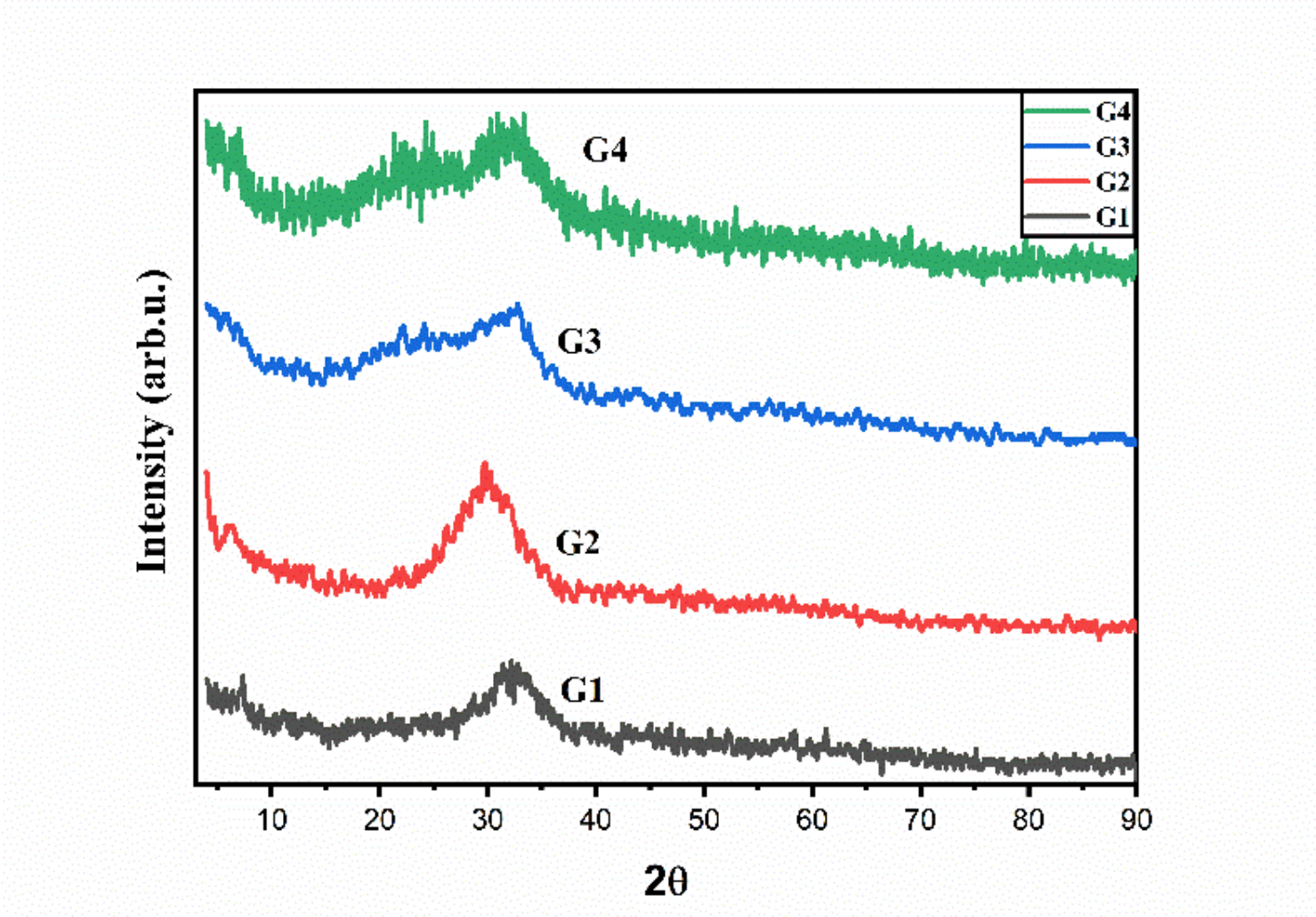

Figure 1

X-ray diffraction of bioglass matrixes sintered at 400 ˚C.

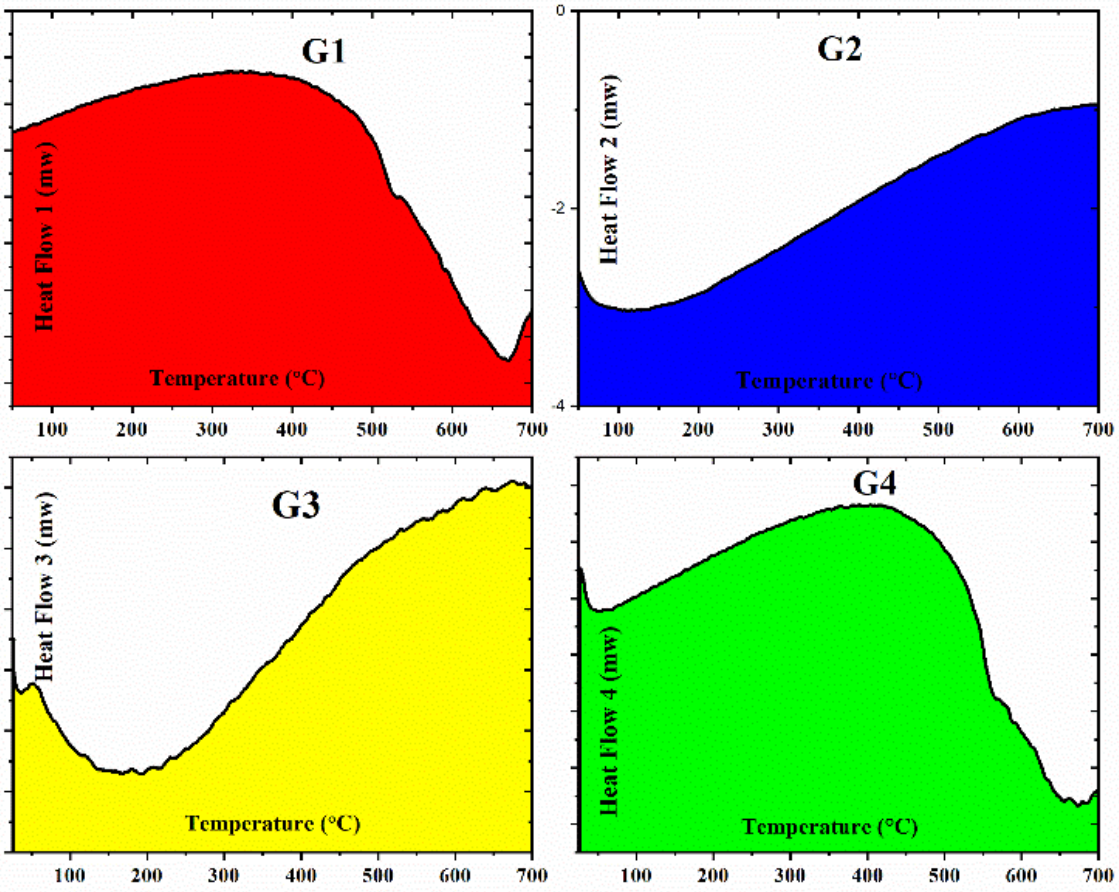

Figure 2

DTA of all studied samples.

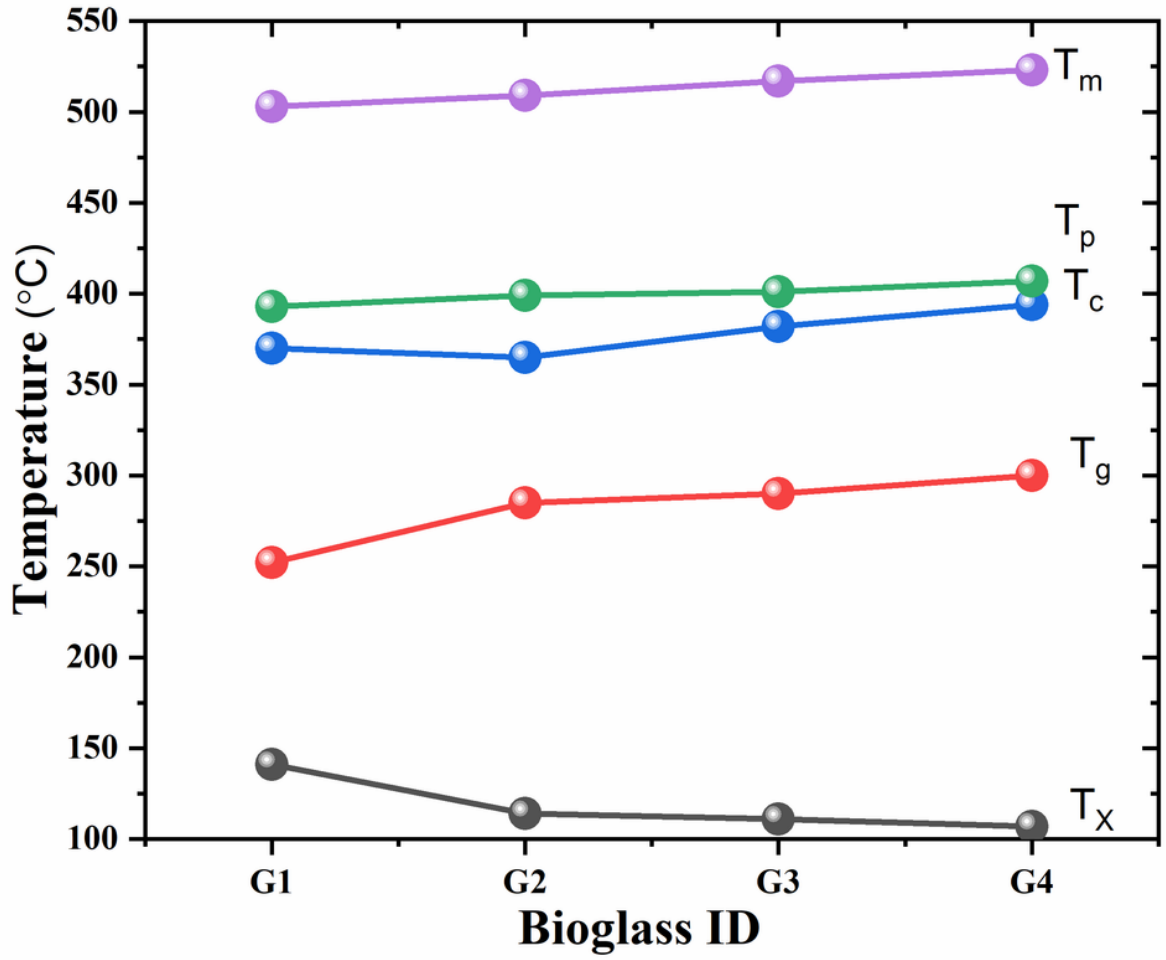

Figure 3

The change of the characteristic temperatures with compositions

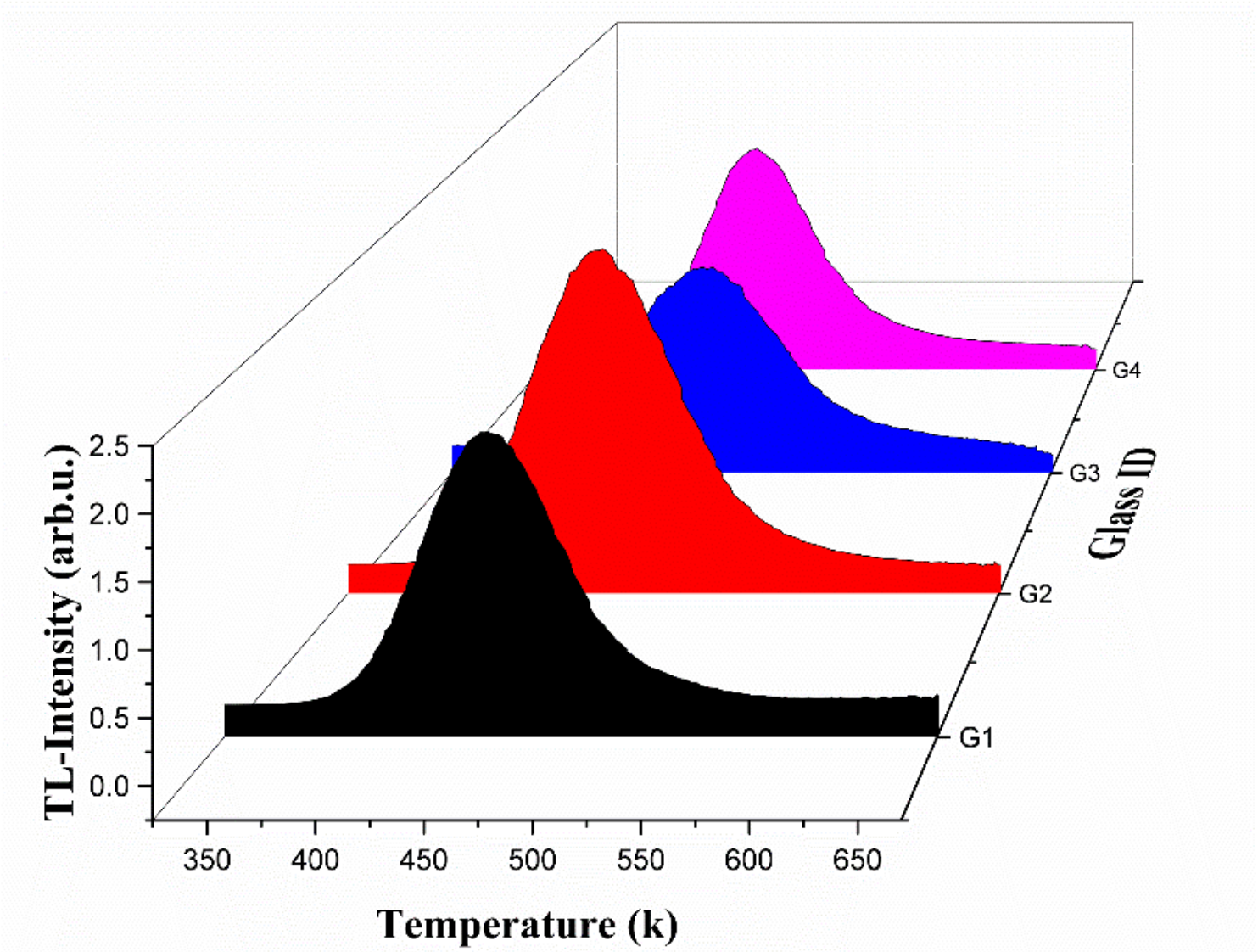

Figure 4

Characteristic glow curves for G1, G2, G3, and G4, respectively.

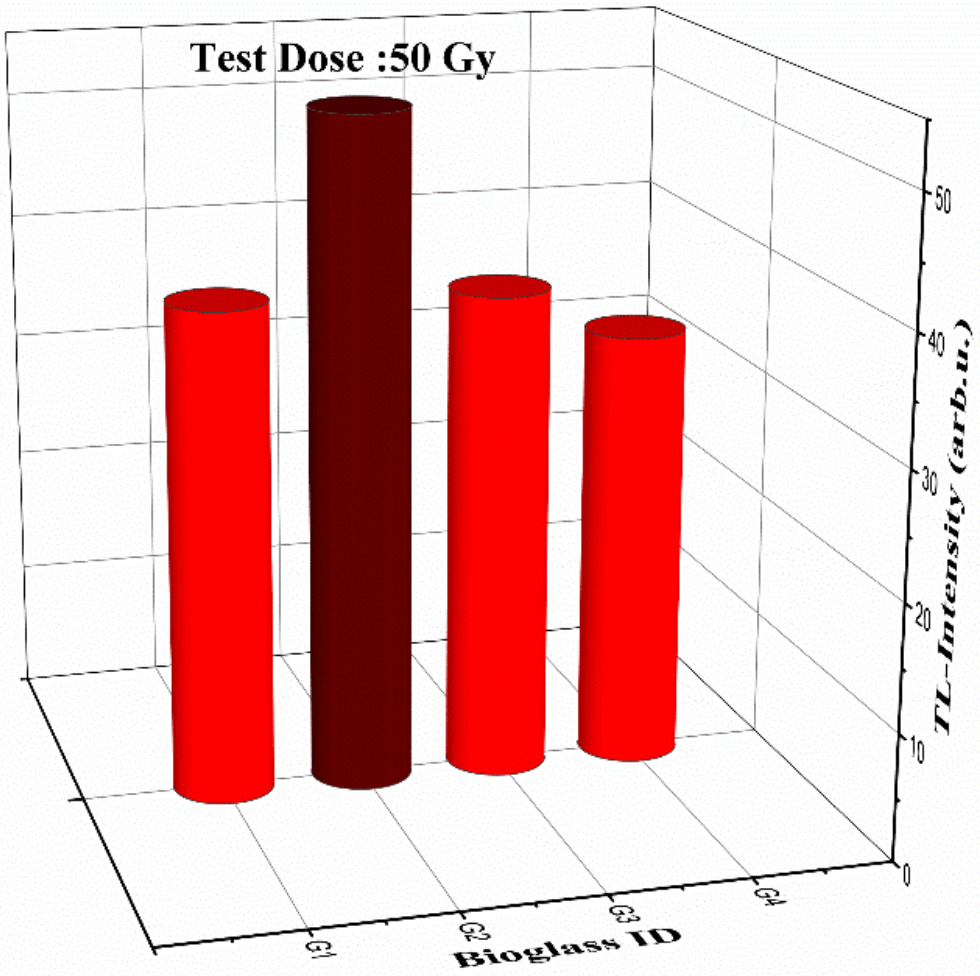

Figure 5

TL-intensity for G1, G2, G3, and G4, respectively.

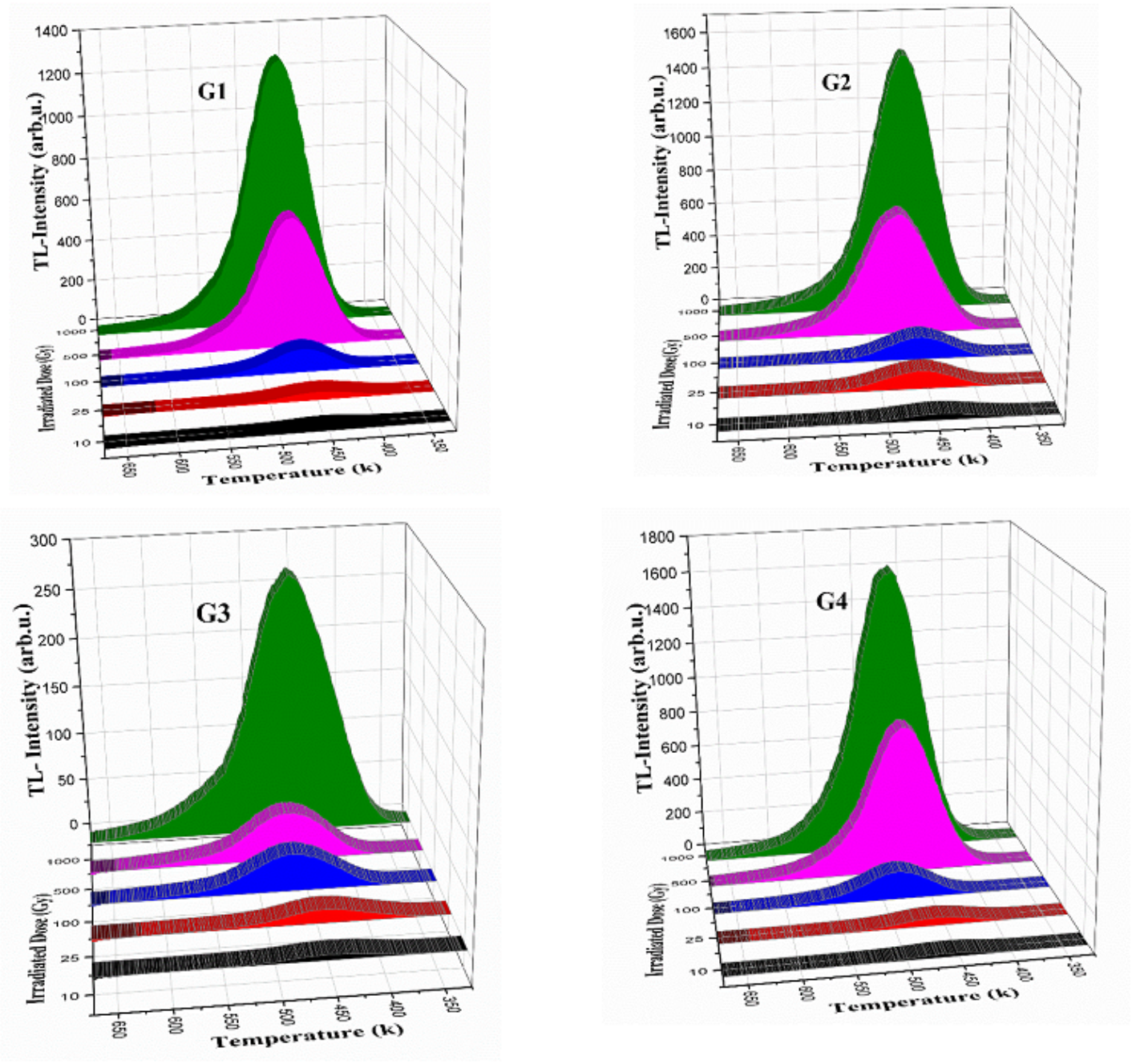

Figure 6

The characteristic glow curve of G1, G2, G3, and G4 respectively after exposed to different gamma doses.

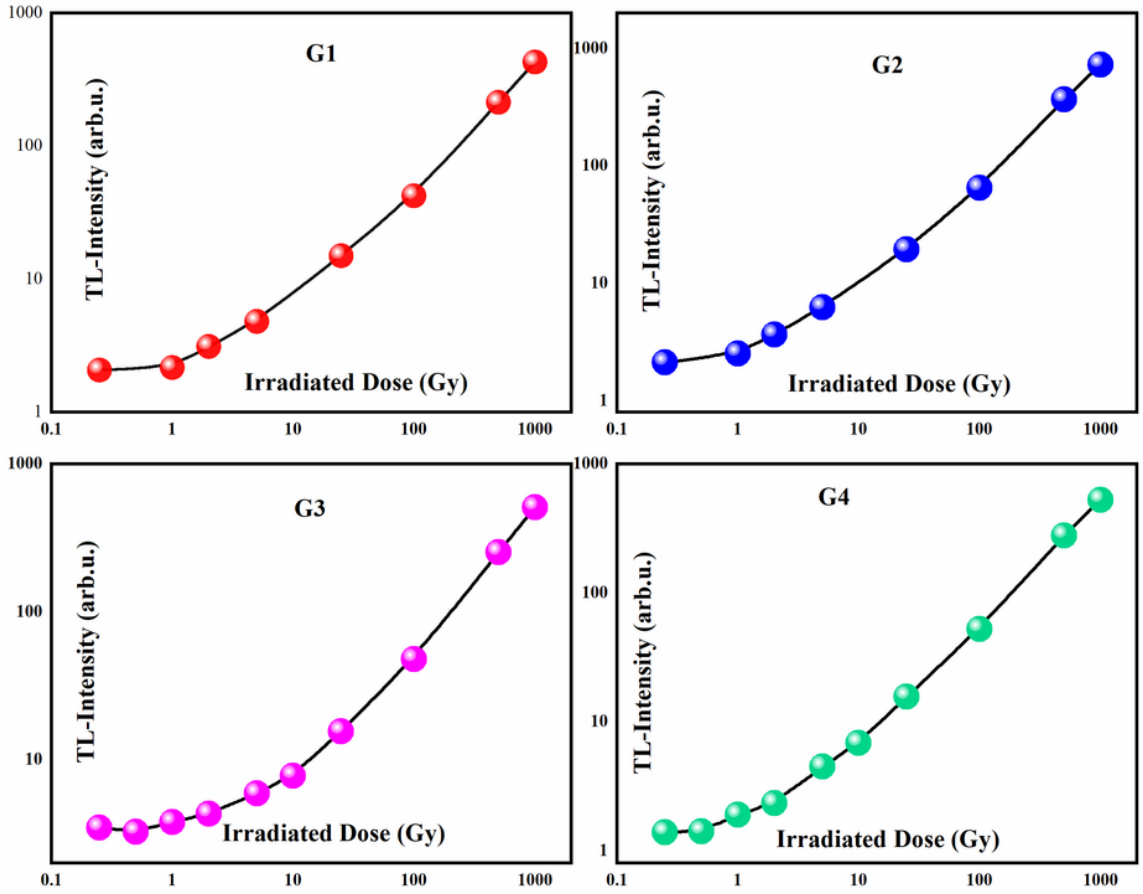

Figure 7

Dose-response curves for G1, G2, G3, and G4, respectively, after exposure to different doses from gamma-ray.

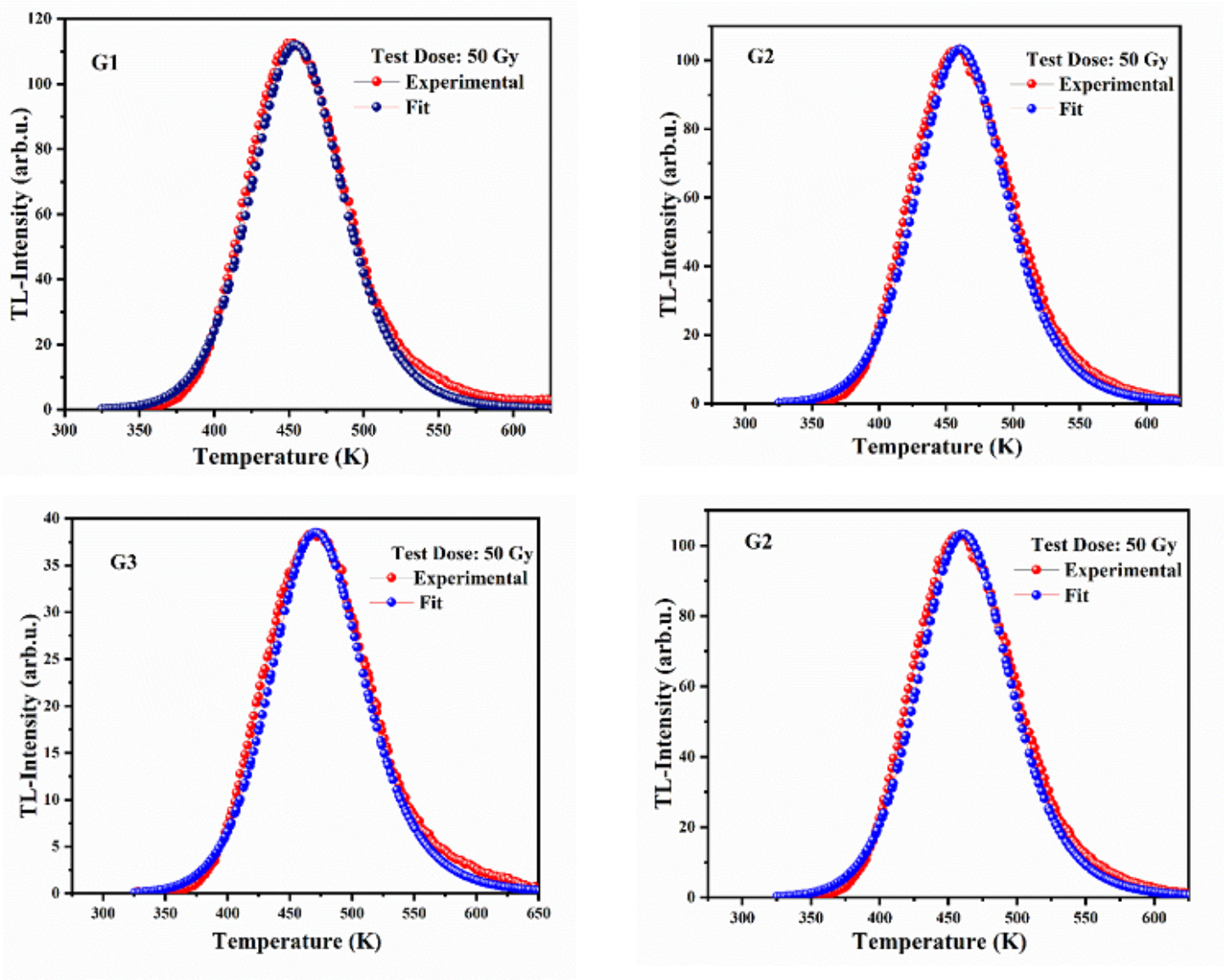

Figure 8

The deconvolution of the glow curves for G1, G2, G3, and, G4 using general orders of kinetics equation derived by kities, et al.,